High levels of m6A methylation and histone acetylation modification patterns contribute to the survival of LUAD patients

LiGuo Jia
ZhenZhen Gao
Jing Chen (chenjing@ncst.edu.cn)

Research Article

Keywords: m6A, histone acetylation, Lung adenocarcinoma, Tumor microenvironment, drug sensitivity

Posted Date: October 28th, 2022

DOI: https://doi.org/10.21203/rs.3.rs-2199422/v1

Abstract

Background

The m6A methylation-regulated histone acetylation modification affects the proliferation and differentiation of mouse embryonic neural stem cells, and recent studies have shown that the deacetylase SIRT1 regulates RNA m6A methylation to promote hepatocellular carcinogenesis. However, the interrelationship between the m6A methylation and histone acetylation, and the potential roles as well as interactions of related regulators in TME cell infiltration and drug sensitivity have not been explored at a holistic level.

Methods

Unsupervised clustering method was used to identify lung adenocarcinoma m6A modification patterns based on 14 m6A regulators and histone acetylation modification patterns based on 37 histone acetylation regulators. Individual samples were then quantified based on their differential gene construction models. Finally, the models were analysed in relation to transcriptional background and TME characteristics to predict potential target drugs and explore the association of m6A methylation with histone acetylation.

Result

Three histone acetylation patterns as well as two m6A methylation patterns were identified. Patients with LUAD in the low-score group had poorer overall survival times and more active cancer-related malignant pathways. m6A methylation was strongly associated with histone acetylation, and high levels of m6A methylation and histone acetylation patients had significantly superior survival and immunoreactivity. VX-680 and GW843682X may be potential drugs available for the low level m6A group.

Conclusion

This work revealed that m6A modifications and histone acetylation modifications have a non-negligible role in the development of TME diversity and complexity. We found that both m6A methylation and histone acetylation are closely associated with tumor malignant pathways. Combined m6A methylation and histone acetylation analysis will help to obtain the understanding of tumor internal regulation and provide new therapeutic directions.

Introduction

Lung cancer is the main cause of cancer deaths in the world. Lung Adenocarcinoma (LUAD) is the main type of Lung cancer, according for approximately 40% of lung cancer patients(1). Clinical indications are

that LUAD is in urgent need of precise treatment. Most LUAD patients are diagnosed with advanced disease due to effective diagnostic methods.Despite advances in treatment methods, the effectiveness of these current treatments remains suboptimal(2).Thus,it is an urgent to explore new prognostic predictors and therapeutic targets for LUAD(3).

There are over 100 known modifications to RNA, and internal modifications to mRNA are used to maintain mRNA stability. mRNA's most common internal modifications include N^6-adenylation (m6A), N^1-adenylation (m1A) etc.m6A modification is a dynamic and reversible process which is regulated by m6A methyltransferases (writers), m6A demethylases (erasers) and m6A- binding proteins (readers) (4).Previous work has shown that m6A acts as a huge role in cancer proliferation, migration and invasion(5).However, the therapeutic effects of m6A modulators and their impact on the prognosis of LUAD need to be further explored. Histone acetylation is a dynamic and reversible post-translational modification whose N-terminal lysine residues can be catalyzed by histone acetyltransferases (HATS) and regulated by proteins that can be divided into three kinds: "writers", "readers" and "erasers". The "writers" are able to transfer acetyl groups to histones, while the "erasers" are able to remove acetyl groups from histones. The "reader" is able to recognize the modified histones(6). As acetyltransferases and transcriptional attackers or substances, HATs have been shown to be related to malignant transformation(7, 8), It regulates the expression of key genes and proteins. HDACs, one of the most studied anticancer targets to date. Histone deacetylase inhibitors (HDACis) can Inhibit the growth of cancer cells and induce differentiation and apoptosis by inhibiting HDAC activity and promoting histone acetylation(9).

In this study, we retrospectively investigated genomic alterations in 2057 LUAD samples from the Cancer Genome Atlas (TCGA) and Gene Expression Omnibus (GEO) cohorts. We comprehensively evaluate histone acetylation modification patterns on the basis of histone acetylation regulators and m6A methylation modification patterns of m6A methylation regulators. We found that the identified modification patterns have different features in terms of activating pathways associated with malignancy and infiltrating multiple immune cells. We also builded model to quantify the histone acetylation patterns and m6A methylation patterns in individual patients.

Materials And Methods

Collection of LUAD Datasets and Preprocessing

The study workflow is shown in **Supplement** Fig. 1. Gene expression data and clinical features of Lung cancer samples were retrospectively retrieved from publicly available datasets of the NCBI GEO database (https://www.ncbi.nlm.nih.gov/geo/) and TCGA (https://portal.gdc.cancer.gov/).Moreover, we obtained genomic mutation data (including somatic mutations and copy number variants) for TCGA-LUAD from the UCSC Xena(https://xenabrowser.net/datapages/). In summary, we analysed 2057 LUAD patients from 8 cohorts: TCGA-LUAD, GSE14814, GSE19188, GSE31210, GSE37745, GSE50081, GSE68465 and GSE72094.Sample names of specific patients can be viewed in **Table S1**.RNA-seq data were converted to

transcripts per kilobase million (TPM) values(10). For microarray data from GEO. Download the original probe expression matrix from GEO and perform RMA dimensionality reduction via “affy” package. Finally, we used the 'Combat' method of the sva package(11) to adjust for batch effects caused by non-biotechnological bias.

Consensus Clustering Expression Pattern

The literature related to histone acetylation, m6A methylation was searched, and 40 histone acetylation genes(12), 22 m6A methylation genes(13) were collated and analysed to identify modification patterns (**Table S2**). Robust clustering of lung adenocarcinoma cancers determined by unsupervised consensus clustering algorithm. We performed the above steps using the R package ConensusClusterplus and performed 1000 replications to ensure classification stability(14).

Gene Set Variation Analysis (GSVA) and Functional Annotation

GSVA enrichment analysis was realized by the "GSVA" R package.(15). The gene sets of "c2.cp.kegg.v7.5.1.symbols" and "c5.go.v7.5.1.symbols" were downloaded from the MSigDB database for GSVA analysis. Some tumor biological features gene signatures obtained from the supplementary table of previous studies.(**Table S3**)(16).The clusterProfiler R package is used for functional annotation of genes, and FDR > 0.05 as the threshold(17).

Estimation of TME cell infiltration

We make use of the single-sample gene-set enrichment analysis (ssGSEA) algorithm and ‘CIBERSORT’ to quantify the relative abundance of each cell infiltration in the LUAD TME. The gene sets defining each immune cell type were obtained from Previous studies(**Table S3**)(18, 19).

Generation of gene signatures

We constructed a score system to quantify the level of m6A methylation and histone acetylation modifications in individual patients, expressed as MAscore versus ACscore. Specifically, as follows, differentially expressed genes were first identified from different gene-clusters, and subsequent selection of prognosis-related genes by univariate Cox regression. Patients were then divided into groups by using an unsupervised clustering approach. Gene expression was then transformed into Z scores and a gene signature was constructed by principal component analysis (PCA). Both principal components 1 and 2 (PC1 and PC2, respectively) were selected as signature scores. This approach focused on the scores of sets with the largest blocks of related (or anti-correlated) genes, while reducing the contribution weights of genes that were not related to other set members. Finally, we used a formula similar to that of previous studies to define the scores.(20, 21):

$$Score = \Sigma(PC1i + PC2i)$$

where i is the expression of modification phenotype-related genes.

Correlation between gene signature and other related biological processes

We evaluated the expression of immune checkpoints. The immunophenotype score (IPS) is a good indicator of tumor immunogenicity, and we downloaded the immunophenotype core (IPS) file from the Cancer Immune Atlas database to assess the significance of gene signatures for immunotherapy. The Tumor Immune Dysfunction and Rejection (TIDE) algorithm. It can effectively reply immune checkpoint blockade responses, with higher scores indicating that tumor cells are more likely to induce immune escape and also indicate a lower response rate to ICI treatment. In our study, the mean of all samples involved in the analysis was used as a normalized control and scores were calculated by applying the Web application(http://tide.dfci.atherard.edu/) with the developer's instructions.

Correlation Analysis of Score and Drug Sensitivity

Based on the Cancer Genome Project (CGP) database, the IC50 of common chemotherapeutic agents was calculated by the 'pRRophetic'(22) software package. Correlations between drug sensitivity and Score were calculated by Spearman's method and considered |Rs|>0.3 and FDR < 0.05 as significant correlations.

Statistical Analysis

In this study R (version 4.1.2) was used to analyse the data. Differences between non-parametric and parametric methods were compared using the Wilcoxon test, Kruskal-Wallis test, t-test or one-way ANOVA. Survminer package to determine the best survival message cutoff for each queue. The score was dichotomized using the surv-cutpoint function. Patients were then categorized into high and low groups, and survival curves for prognostic analysis were assessed using the Kaplan-Meier method with a log-rank test to assess between-group differences. we included the score and associated clinical parameters in a multivariate Cox regression model analysis. Statistical significance was set at $P < 0.1$, and significance was set at $P < 0.05$.

Results

Genetic and Transcriptional Alterations of Histone Acetylation Regulators and m6A Regulators in LUAD

Reviewing published articles, A total of 57 genes regulated by m6A methylation and histone acetylation that were included in the analysis. Metascape analysis was performed on these genes. The biological processes that significantly enriched were mainly associated with histone modification, epigenetics and others, as summarized in Figs. 1A.Based on 57 regulators, LUAD samples were well separated from normal samples. (Figs. 1B). We evaluated the somatic mutation rates of the two groups of regulators separately to identify genetic changes of the regulators in cancer. In the LUAD cohort of TCGA, 121 of 527 samples (22.96%) experienced alterations in m6A methylation regulatory genes, while 195 (37%) experienced alterations in histone acetylation regulatory genes. The highest mutation rates were found in ZC3H13 (4%) and HDAC9 (6%) respectively (Figs. 1C, D). A survey of CNV variation frequencies showed

that CNV variation was prevalent in 57 regulatory genes and mostly concentrated in copy number amplification, while CNV deletion frequencies were prevalent in genes such as ZX3H13, SIRT5 and BRDT (Figs. 1E). The location of CNV alterations in regulatory factors on chromosomes is shown in Figs. 1F. We also investigated the expression of regulatory factors in LUAD and normal lung tissues and found differences in the expression of the vast majority of genes. The above analysis showed the genetic and expression changes of 57 regulators were highly heterogeneous between LUAD and normal tissues (Figs. 2A, B), suggesting that the unbalanced expression of these regulators profoundly affects the development of LUAD. Furthermore, genes do not function in isolation; therefore, we explored the correlation between m6A regulators and histone acetylation regulators. We found that the mRNAs of both are highly correlated in expression (Figs. 2C). These imply a tight crosstalk between and within histone acetylation regulators and m6A methylation regulators. m6A methylation and histone acetylation regulators have highly heterogeneous genetic and expression patterns between LUAD and normal samples, also suggesting that regulators are critical for the development of LUAD.

Identification of Two m6A Methylation Modification Patterns and Three Histone Acetylation Modification Patterns

14 m6A methylation regulators and 37 histone acetylation regulators were used for further analysis of the corresponding expression patterns based on mRNAs from 2057 lung adenocarcinoma patient samples from TCGA-LUAD, GSE14814, GSE19188, GSE31210, GSE37745, GSE50081, GSE68465 and GSE72094. To identify the expression patterns of regulatory factors, mRNA expression data from LUAD samples were classified using ConsensusClusterPlus. Using unsupervised clustering, we identified two m6A methylation patterns with different properties (Figs. 3A), including 1322 cases of cluster A, 735 cases of cluster B. We named these patterns as MAclusterA, MAclusterB. Three histone acetylation patterns with different properties, including 170 cases of cluster A, 1071 cases of cluster B, 816 cases of cluster C (Figs. 3B), were termed as ACclusterA-C. Combined with the survival information of the samples, the prognostic analysis showed that the m6A methylation subgroup had a better survival in the MAclusterB group than MAclusterA group (Figs. 3C). Among the three subgroups with histone acetylation modification patterns, AClusterA had a better probability of survival in the first 7 years, and AClusterB had the worst probability of survival (Figs. 3D). Notably, tSNE analysis showed significant differences in transcriptional profiles among m6A methylation modification patterns and the three histone acetylation modification patterns, respectively(Figs. 3E, F), which also indicated the success of our unsupervised clustering results. Finally, we grouped 2057 samples according to the grouping of m6A methylation with histone acetylation and performed survival analysis. the common sample group of MAclusterB and AClusterB had better survival, while interestingly: Samples in the AClusterC group, which had a higher survival rate and also belonged to the MAclusterA group, which had a low survival rate, instead had a lower survival rate than those in the AClusterB group, which also belonged to the MAclusterA group and had a lower survival rate. Subsequently, we obtained similar results in TCGA-LUAD and GEO meta cohort(**Supplement** Figs. 2).

Molecular Background of Tumors and Infiltration Characteristics of TME Cells in Different Patterns

To identify the differences in biological behavior between the different modification patterns of m6A methylation and histone acetylation, GSVA enrichment analysis was performed (**Table S4, Figs. 4A, B Supplement** Fig. 3A-C). MAclusterA was enriched in cancer pathways MYC/NOTCH/PI3K/TGF-Beta, and cell cycle, while MAclusterB was enriched in Antigen processing machinery/WNT/EMT/Angiogenesis/CSCs activity pathways (Figs. 4C). In the histone acetylation pattern, the highest abundance in the cell cycle/HIPPO/MYC/NOTCH/PI3K/TGF-Beta pathway was in the AClusterB group and the lowest in the AClusterA group, while the highest abundance in the WNT/EMT/Angiogenesis pathway was in the AClusterC. interestingly, in the lowest abundance in the EMT and CSCs activity pathway was in the AClusterA group rather than in the AClusterB group, which had the worst survival rate (Figs. 4D). These results reflect that the regulatory pattern is closely related to the biological behavior of lung adenocarcinoma. Highly active regulators may be a key factor in improving the malignancy of lung adenocarcinoma.

In previous studies, immune cell infiltration of TME was significantly correlated with alterations in histone acetylation and m6A methylation. Therefore, we analyzed the role played by 57 regulators in TME. The relative abundance of infiltrating TME immune cells was quantified by ssGSEA algorithm **(Supplement** Fig. 3D, E**)** and "CIBERSOFT" package **(Supplement** Fig. 3F, G**)**. And the association between regulators and TME-infiltrating immune cells was analyzed (Figs. 4E, **F**). Evaluation of tumor purity of samples with 'ESTIMATE' package (**Supplement** Fig. 3H-N). T cells gamma delta, Mast cells resting, Eosinophils and Immature. dendritic.cells were positively correlated with the majority of regulatory factors. We also analyzed the TME cell infiltration in various patterns. MAclusterB differed significantly from MAclusterA. The abundance of plasmacytoid dendritic cells was higher in MAclusterB than in MAclusterA, suggesting that MAclusterB has a higher antigen-presenting function. Natural killer cells, immature dendritic cells, etc., were in higher abundance in MAclusterB. However, activated CD8 T cells, the most potent effector in the anticancer immune system(23), as well as other important tumor-killer cells and gamma delta T cells (24), were lower in MAclusterB than in MAclusterA(Figs. 4G).In the histone acetylation pattern(Figs. 4H), plasmacytoid dendritic cells were much more abundant in the ACclusterC than in the ACclusterB group. Natural killer cells were equally abundant in AC group C than in AC group B. Similar to m6A methylation, the abundance of Activated CD8 T cell, Gamma delta T cell and other cells were higher in the ACclusterB group. What is interesting is the ACclusterA group. It has comparable levels of Regulatory T cell, Macrophage, Natural killer cell, Natural killer T cell with the ACclusterC group, and also has comparable levels of Activated CD8 T cell with the ACclusterB group. B cell abundance in the ACclusterA group was much higher than that in ACclusterB and ACclusterC, and also had the lowest abundance of Activated CD4 T cell. These results suggest that the modification patterns of both m6A methylation and histone acetylation are closely related to the tumor immune microenvironment.

Based on the analytical results of our study and the experimental findings of previous authors. We selected FTO, KAT2B, METTL3 for further analysis (Figs. 4E, **F**). We divided the samples into a high FTO group and a low FTO group by FTO expression. k-M plot analysis showed high FTO expression group had better survival, and we subsequently examined the expression levels of m6A methylation and histone acetylation regulators in both groups and found that the expression of regulators in the high FTO group

far exceeded that in low group (**Supplement Fig. 4A, B**). We also obtained the same results in the corresponding analysis of two genes, KAT2B, METTL3(**Supplement Fig. 4C-F**). Lin et al, noted that METTL3 promotes translation in human lung adenocarcinoma. We therefore collected genome-wide mRNA expression data from GSE200649 transfected with shMETTL3 versus NC in control cells. The expression differences between m6A methylation regulators and histone acetylation regulators after transfection were analyzed. Interestingly, in this dataset, the difference in expression of stably transfected shMETTL3 at the mRNA level was not significant (**Table S5**). These results further suggest a tight relationship between m6A methylation regulators and histone acetylation regulators.

Identification of phenotype-related genes

Due to the differences in regulatory transcriptional profiles between m6A modification Pattern as well as histone acetylation modification Pattern, we then explored the genetic variation and mechanisms of the congregational modification patterns. Identification of differential genes between subgroups by limma R package. We identified DEGs between the MAclusterA and MAclusterB groups and between the AClusterA, AClusterB and AClusterC groups (**Table S6**). Subsequently, 18 and 27 genes associated with survival were selected respectively. To further deepen the understanding of m6A methylation and histone acetylation, Unsupervised clustering analysis was performed with 18 and 27 genes separately and patients were classified into different gene clusters. As with previous modification patterns, two m6A-modified gene phenotypes and three histone acetylation-modified gene phenotypes were identified. (Fig. 5A, B). We named them as MA-gene-clusterA/B, AC-gene-clusterA/B/C, respectively. These results suggest that three histone acetylation modification modes and two m6A methylation modification modes do exist in LUAD. A significant proportion of genes in the m6A gene cluster pattern are highly expressed in MA-gene-clusterB. We then performed unsupervised clustering of the TCGA cohort separately from the meta-GEO cohort (**Supplement** Fig. 5A-F). It was found that the samples were still clustered into two groups. The same clustering was also used to analyze the histone acetylation gene cluster patterns (Fig. 5C, D), with the AC-gene-clusterA group having the highest expression of PRMT1, RHOB and TAF10, while all other DEGs had lower expression than that both in AC-gene-clusterB and AC-gene-clusterC groups. The expression levels of DEGs in the better surviving AC-gene-clusterC were higher than those in AC-gene-clusterB group. Subsequently, we analyzed the expression of m6A and histone acetylation regulators in the gene cluster. Notably, The expression of m6A methylation regulators was also much higher in the AC-gene cluster C group than in the AC-gene-cluster-B group. The expression level of m6A methylation regulators in AC-gene-clusterC group was also significantly higher than that in AC-gene-clusterB group (Fig. 5E-G). Similarly, the expression of 57 regulators in the MA-gene-cluster was higher in MA-gene cluster B than in MA-gene cluster A(Fig. 5H-J).To reveal the role of related phenotypes in TME immunomodulation, we investigated the expression of chemokines and cytokines in gene clusters. Cytokines and chemokines were extracted from the published literature(25, 26). Interestingly: TGFb/EMT pathway-related mRNAs, immune activation transcript-related mRNAs and immune checkpoint-related mRNAs were all highly expressed in MAgA.ACgC(The group consisting of MA-gene-clusterA and AC-gene-clusterC common samples) and MAgB.ACgC (The group consisting of MA-gene-clusterB and AC-gene-clusterC common samples)groups(**Supplement** Fig. 5G-I).The ssGSEA analysis showed that MAgA.ACgC

and MAgB.ACgC were more active in the pathways of Antigen processing machinery, EMT and CSCs activity. Consistent with our previous findings (**Supplement** Fig. 5J**)**

Construction of a Digital Model for Individual Lung Adenocarcinoma Patients

Patients with lung adenocarcinoma are heterogeneous and complex. We constructed a phenotypic gene-based scoring model, called MAscore and ACscore, respectively. The variation of patients' attributes can be clearly observed by alluvial plots (Fig. 6A, **Supplement** Fig. 6A, B). We analyzed the correlation between the scores and immune cells, Type 2 T helper cell, Eosinophil, Immature dendritic cell and Mast cell were significantly positively correlated with MAscore, while Gamma delta T cell and CD56dim. Natural killer cells were significantly negatively correlated with MAscore. Type 2 T helper cell, Eosinophil and Immature dendritic cell are significantly positively correlated with ACscore, while CD56dim natural killer cell and Monocyte are significantly negatively correlated with ACscore(Fig. 6B,**Supplement** Fig. 6C).Then, we analyzed the scores in cluster and gene-cluster. The MAclusterB and MA-gene-clusterB groups with better survival had much higher MAscore than the MAclusterA and MA-gene-clusterA groups, respectively (Fig. 6C, D). While the ACscore in the subgroup of histone acetylation, ACclusterA, which had a better survival curve among ACcluster and AC-gene-cluster, AC-gene-clusterA had the lowest ACscore score among the respective groups. The ACscore of ACclusterC and AC-gene-clusterC with better survival was higher than that of ACclusterB and AC-gene-clusterB with poorer survival, respectively (Fig. 6E, F). Cox regression analysis in the TCGA cohort showed that our constructed MAscore and ACscore can be used as independent prognostic detectors. Using the optimal cut-off point to classify patients into high and low groups, survival analysis showed that patients with high scores had a better survival prognosis than patients with low scores. Combining the high and low groups of m6A methylation and histone acetylation, the survival analysis showed that the group with both MAscore and ACscore had better survival, and encouragingly, the expression levels of m6A regulators and histone acetylation regulators in this group far exceeded those of other lung adenocarcinoma patients (Fig. 6G, H).

Models predict potential therapeutic drugs

Based on the Cancer Genome Project (CGP) database, we predicted the sensitivity of 138 drugs. We selected drugs with lower IC50 values in the low-risk group in the m6A methylation and histone acetylation subgroups, and selected drugs with higher IC50 values in both the MASH.ACSH group than in the other groups, followed by analysis of the drugs most associated with MAscore, ACscore values.GW843682X, MS.275, S.Trityl.L.cysteine. VX.680 were screened (Fig. 7A, **Table S7**). gw843682X is a PLK inhibitor that plays a role in regulating cell mitosis, etc. MS.275 is a histone deacetylase inhibitor that potently inhibits HDAC1 and HDAC3. s.Trityl.L.cysteine is an Eg5 inhibitor that induces mitotic arrest in HL-60 cells and VX.680 is an inhibitor of pan-Aurora, which is also a regulator of mitosis. We analyzed the expression of the target genes of the four drugs in each risk group, in which AURKB and PLK1 may be effective therapeutic targets(Fig. 7B), and then analyzed the relationship between the expression of AURKB, PLK1 and LUAD survival, survival analysis showed better survival in patients with low levels of AURKB and PLK1(Fig. 7C,D), which also reflects that VX.680, GW843682X may be a promising drug for

the treatment of patients in MASL.ACSH and MASL.ACCSL groups. TIDE, which is widely used and highly recommended for assessing immune responses in cancer-related studies(27, 28). Considering the MAscore, the ACscore seems to be closely related to TME. We analyzed the differences in TIDE scores across subgroups. The results showed that the TIDE scores of MASH. ACSL were much lower than those of the MASH.ACSL and MASL.ACSL groups (Fig. 7E). However, the MASH.ACSH group did not have the lowest scores, but rather the MASL.ACSH group had the lowest TIDE scores, and it is possible that the MASL.ACSH group had a higher treatment outcome from ICI treatment. Therefore, we explored the correlation between MAscore /ACscore and immunophenoscore (IPS) in LUAD for the purpose of predicting the response of immune checkpoint inhibitors (ICIs). Correlation analysis showed that MAscore, ACscore and ips_ctla4_neg_pd1_pos, and ips_ctla4_pos_pd1_pos had the highest negative correlation (Fig. 7F). The expression of immune checkpoints were similarly higher in the MASH.ACSH group than in the others. This likewise reflects the high level of m6A methylation with high immunoreactivity of histone acetylation (Fig. 7G).

Organelle division aids m6A methylation and histone acetylation to identify LUAD patients with better prognosis

In a previous study (Fig. 3I), we found that the m6AA.AcC group, which should have survived better, instead had a worse survival curve than the m6AA.AcB group. Not coincidentally, the MAgA.ACgC group in the genome had better survival than the MAgB.ACgC group instead. We extracted these patients for further analysis. Survival analysis showed no significant difference between m6AA.AcB and m6AA.AcC (Fig. 8A), while MAgA.ACgC, MAgB.ACgC survival differed significantly (Fig. 8B). Interestingly, when we analyzed the expression of m6A methylation regulators and histone acetylation regulators in these groups, we found no significant survival differences between the m6AA.AcB and m6AA.AcC groups, but instead there were considerable differences in the expression levels of the regulators (Fig. 8C, D), while there were mostly no significant differences in the expression of the regulators between MAgA.ACgC and MAgB.ACgC group (**Supplement** Fig. 7A, B). This result predicts the existence of one or more pathways that effectively assist in the modification pattern of m6A methylation and histone acetylation. To explore whether such a pathway exists, we performed differential analysis of the two groups, MAgA.ACgC and MAgB.ACgC, and identified a total of 235 differential genes. We then performed GO and KEGG enrichment analysis based on these 235 genes. Most of the enrichment results were associated with cell proliferation (**Table S8**). We selected 6 biological features for further analysis. The activity of each sample pathway was quantified by GSVA and was significantly higher in the MAgA.ACgC group than in the MAgB.ACgC group in five biological features (Fig. 8E). Based on a total of 1152 samples from the MAgA.ACgC and MAgB.ACgC groups, we found that the lower the activity of the four pathways CELL CYCLE, CHROMOSOME SEGREGATION, MITOTIC NUCLEAR DIVISION and ORGANELLE FISSION, the higher the survival rate (**Supplementary Fig. 7C-H**). We then introduced ORGANELLE FISSION into the grouping of m6A methylation with histone acetylation. Survival analysis showed that ORGANELLE FISSION complemented the grouping of m6A methylation and histone acetylation (Fig. 8F, **Supplementary Fig. 7I, L**), and the expression levels of most m6A methylation and histone acetylation regulators were also significantly different (Fig. 8E, F).

Discussion

Much evidence suggests that m6A regulators play an integral role in inflammation, innate immunity, and antitumor. However, most studies have targeted only single factors, and progress in the overall role of m6A regulators remains relatively slow. Histone acetylation faces a similar situation, and relatively little is known about the relationship between the roles of these regulators ("writers", "erasers" and "readers") in cancer. Because epigenetic modifications are a tight network, a holistic analysis is necessary in cancer research. hunag et al. revealed crosstalk between histone modifications and RNA methylation(27). And Liu et al. further revealed that SIRT1 can promote SUMOization of m6A demethylase, which in turn increases m6A modification of the oncogene GNAO1 and other hepatocellular carcinoma-related genes, leading to the development of hepatocellular carcinoma(29), all of which suggest a strong intrinsic link between histone acetylation and m6A methylation. Determining the pattern of m6A modification and histone acetylation modification will improve our understanding of tumorigenesis development and guide clinical progression.

In this study, A total of 57 regulators related to m6A methylation and histone acetylation, the expression of almost all regulators were positively correlated with each other and the correlation coefficients were extremely high. Based on 14 m6A methylation regulators and 37 histone acetylation regulators, we classified patients into two m6A methylation phenotypes and three histone acetylation phenotypes, respectively (MAclusterA/MAclusterB, ACcluster A/ACcluster B/ACcluster C). The expression of 14 m6A methylation regulators was much higher in the MAclusterB group than in MAclusterA group, and K-M plot also advised the MAclusterB group had a much better survival than the MAclusterA group. 37 histone acetylation regulators were over-expressed in the AClusterC group than in the AClusterB group, and survival The survival analysis was also better in the AClusterC group. In the AClusterA group, the expression of 19 of the 37 histone acetylation regulators were significantly higher in the AClusterA group than in the AClusterB group, and the expression levels of 13 regulators were lower in the AClusterA group than in the AClusterB group. Survival analysis showed that AClusterA had the highest survival rate at 2–7 years. To explore the mechanisms responsible for the differences in prognosis of patients with different phenotypes, we first analyzed the biological features of cancer using m6A methylation and histone acetylation patterns. We found that the MAclusterA group was characterized by cell cycle, HIPPO(30),MYC,NOTCH(31),PI3K and TGF-Beta(32) were significantly activated. These pathways are critical in tumor development, several pathways had the highest activity in the AClusterB group, followed by the AClusterC group and the lowest in the AClusterA. the EMT, Angiogenesis, and CSCs activity pathways had the highest activity in the AClusterC group. these pathways also had the highest activity in the AClusterB group, followed by the AClusterC group and the lowest in the AClusterA. the EMT, Angiogenesis, and CSCs activity pathways had the highest activity in the AClusterC group. Common differential genes between the DEGs located between MAcluster A and MAcluster B and between the AClusterA, ACluster and AClusterC groups were identified by analyzing the transcriptional patterns of related genes. These DEGs were designated as phenotypically related marker genes. Key genes associated with survival were screened by Cox regression analysis and a scoring system was established with 18 and 27 genes to assess the modification pattern of individual LUAD patients, respectively.

VX-680 is an inhibitor that targets Aurora kinase(33).VVX-680 inhibits cell proliferation and induces apoptosis in many cancer types(34, 35). In addition, VVX-680 enhances the chemosensitivity of cisplatin(36). GW843682X is an inhibitor of PLK1(37).GW843682X is capable of inhibiting the G2/M checkpoint(38).However, GW843682X also had an inhibitory effect on the kinase activity of PLK3. In lung adenocarcinoma, PLK3 expression is down-regulated and much higher in the MASH.ACSH group with better survival, so it may be difficult to achieve full success when treating lung adenocarcinoma patients with GW843682X, and combining other drugs or treatment modalities to eliminate the inhibition of PLK3 may yield surprising results. The tumor immune dysfunction and exclusion (TIDE) algorithm is a modeling approach that effectively predicts the immune checkpoint blockade response, and the TIDE score largely reflects the likelihood of tumor immune escape. The higher TIDE scores in MASL.ACSH and MASL.ACSH groups indicate that samples in these two groups are more likely to develop immune escape. vX-680 and GW843682X are the drugs targeted to MASL.ACSH and MASL.ACSH groups. It is likely that these two drugs play some inhibitory role in immune escape.

Finally, consider that we found in the previous analysis that the survival of some subgroups was not exactly as expected. We used the MAgA.ACgC and MAgB.ACgC groups with significant survival differences as a breakthrough and found that several biological features and pathways were closely related to the differential genes in these two groups. Further analysis revealed that biological features such as organelle division could effectively assist in the classification of patients by m6A methylation and histone acetylation modification patterns. This also reflects the important role of m6A methylation and histone acetylation in the development of lung adenocarcinoma, and the crosstalk between the two reflects the complex regulatory mechanisms within tumor cells, and increasingly illustrates the importance of the overall analysis of tumor cells.

Conclusion

In this study, we identified a histone modification pattern based on 37 histone acetylation regulators and a m6A methylation modification pattern based on 14 m6A methylation regulators. Systematic analysis showed that the high mortality in the group with poorer survival may be due to high tumor malignant pathway activity. Based on the transcriptional differences between phenotypes, we constructed a score model to numerically describe lung adenocarcinoma patients and identified potential drugs for the poorly scored group. In conclusion, our study suggests that combining m6A methylation with histone acetylation to assess patients will enhance our understanding of the TME profile and help develop, combined and immune-targeted treatment strategies for LUAD patients. In brief, we have established that m6A methylation modifications and histone acetylation modifications interact with each other, and our study also shows that m6A methylation and histone acetylation alone cannot fully analyse the situation of lung adenocarcinoma patients, and that more biological characteristics and deeper exploration remain to be enhanced. However, our study also suffers from limitations such as lack of experimental validation and incomplete clinical data on patients.

Abbreviations

TME Tumor microenvironment

m6A N6-methyladenosine

LUAD Lung adenocarcinoma

m1A N1-adenylation

TIDE The Tumor Immune Dysfunction and Rejection

IPS The immunophenotype score

ICI Immune checkpoint inhibitors

CGP Cancer Genome Project

CNV copy number variation

M6AA.AcA A grouping consisting of common samples of MAclusterA and ACclusterA groups.M6AA.AcB, M6AA.AcC, M6AB.AcB and M6AB.AcC are similar.

MASH.ACSH A grouping consisting of common samples from the MAscore high group and the ACscore group.MASH.ACSL,MASL,ACSH and MASL,ACSL are similar.

Declarations

Acknowledgments

We sincerely thank TCGA and GEO database for providing the platform and contributors for uploading the data. The platform is provided and we thank the contributors for uploading their meaningful datasets. We would like to thank "Brother Sangxin" for sharing his R learning experience.

Author information

Authors and Affiliations

College of Life Sciences, North China University of Science and Technology, 21 Bohai Road, Caofeidian Xincheng, Tangshan 063210, Hebei, China.

LiGuo Jia , ZhenZhen Gao , Jing Chen

Contributions

JLG provides ideas and main data analysis, GZZ is responsible for data review and participation in article writing, and CJ is responsible for article review.

Corresponding author

Correspondence to Jing Chen.

Conflicts of Interest

All authors declare no conflicts of interest.

Funding

This work was supported by the Natural Science Foundation of Hebei Province (H2021209004)

References

1. Shi J, Hua X, Zhu B, Ravichandran S, Wang M, Nguyen C, et al. Somatic Genomics and Clinical Features of Lung Adenocarcinoma: A Retrospective Study. PLoS Med. 2016;13(12):e1002162.
2. Zheng M. Classification and Pathology of Lung Cancer. Surg Oncol Clin N Am. 2016;25(3):447–68.
3. Mangogna A, Belmonte B, Agostinis C, Zacchi P, Iacopino DG, Martorana A, et al. Prognostic Implications of the Complement Protein C1q in Gliomas. Frontiers In Immunology. 2019;10:2366.
4. Yang Y, Hsu PJ, Chen Y-S, Yang Y-G. Dynamic transcriptomic mA decoration: writers, erasers, readers and functions in RNA metabolism. Cell Res. 2018;28(6):616–24.
5. Liu Z-X, Li L-M, Sun H-L, Liu S-M. Link Between m6A Modification and Cancers. Front Bioeng Biotechnol. 2018;6:89.
6. Sabari BR, Zhang D, Allis CD, Zhao Y. Metabolic regulation of gene expression through histone acylations. Nat Rev Mol Cell Biol. 2017;18(2).
7. Ell B, Kang Y. Transcriptional control of cancer metastasis. Trends Cell Biol. 2013;23(12):603–11.
8. Farria A, Li W, Dent SYR. KATs in cancer: functions and therapies. Oncogene. 2015;34(38):4901–13.
9. Autin P, Blanquart C, Fradin D. Epigenetic Drugs for Cancer and microRNAs: A Focus on Histone Deacetylase Inhibitors. Cancers (Basel). 2019;11(10).
10. Wagner GP, Kin K, Lynch VJ. Measurement of mRNA abundance using RNA-seq data: RPKM measure is inconsistent among samples. Theory Biosci. 2012;131(4):281–5.
11. Leek JT, Johnson WE, Parker HS, Jaffe AE, Storey JD. The sva package for removing batch effects and other unwanted variation in high-throughput experiments. Bioinformatics. 2012;28(6):882–3.
12. Dai Q, Ye Y. Development and Validation of a Novel Histone Acetylation-Related Gene Signature for Predicting the Prognosis of Ovarian Cancer. Front Cell Dev Biol. 2022;10:793425.
13. Sun T, Wu R, Ming L. The role of m6A RNA methylation in cancer. Biomed Pharmacother. 2019;112:108613.

14. Wilkerson MD, Hayes DN. ConsensusClusterPlus: a class discovery tool with confidence assessments and item tracking. Bioinformatics. 2010;26(12):1572–3.
15. Hänzelmann S, Castelo R, Guinney J. GSVA: gene set variation analysis for microarray and RNA-seq data. BMC Bioinformatics. 2013;14:7.
16. Mariathasan S, Turley SJ, Nickles D, Castiglioni A, Yuen K, Wang Y, et al. TGFβ attenuates tumour response to PD-L1 blockade by contributing to exclusion of T cells. Nature. 2018;554(7693):544–8.
17. Yu G, Wang L-G, Han Y, He Q-Y. clusterProfiler: an R package for comparing biological themes among gene clusters. OMICS. 2012;16(5):284–7.
18. Thorsson V, Gibbs DL, Brown SD, Wolf D, Bortone DS, Ou Yang T-H, et al. The Immune Landscape of Cancer. Immunity. 2018;48(4).
19. Bindea G, Mlecnik B, Tosolini M, Kirilovsky A, Waldner M, Obenauf AC, et al. Spatiotemporal dynamics of intratumoral immune cells reveal the immune landscape in human cancer. Immunity. 2013;39(4):782–95.
20. Sotiriou C, Wirapati P, Loi S, Harris A, Fox S, Smeds J, et al. Gene expression profiling in breast cancer: understanding the molecular basis of histologic grade to improve prognosis. J Natl Cancer Inst. 2006;98(4):262–72.
21. Zhang B, Wu Q, Li B, Wang D, Wang L, Zhou YL. mA regulator-mediated methylation modification patterns and tumor microenvironment infiltration characterization in gastric cancer. Mol Cancer. 2020;19(1):53.
22. Geeleher P, Cox N, Huang RS. pRRophetic: an R package for prediction of clinical chemotherapeutic response from tumor gene expression levels. PLoS One. 2014;9(9):e107468.
23. Raskov H, Orhan A, Christensen JP, Gögenur I. Cytotoxic CD8 T cells in cancer and cancer immunotherapy. Br J Cancer. 2021;124(2):359–67.
24. Ma R, Yuan D, Guo Y, Yan R, Li K. Immune Effects of γδ T Cells in Colorectal Cancer: A Review. Frontiers In Immunology. 2020;11:1600.
25. Barbie DA, Tamayo P, Boehm JS, Kim SY, Moody SE, Dunn IF, et al. Systematic RNA interference reveals that oncogenic KRAS-driven cancers require TBK1. Nature. 2009;462(7269):108–12.
26. Zeng D, Li M, Zhou R, Zhang J, Sun H, Shi M, et al. Tumor Microenvironment Characterization in Gastric Cancer Identifies Prognostic and Immunotherapeutically Relevant Gene Signatures. Cancer Immunol Res. 2019;7(5):737–50.
27. Huang H, Weng H, Zhou K, Wu T, Zhao BS, Sun M, et al. Histone H3 trimethylation at lysine 36 guides mA RNA modification co-transcriptionally. Nature. 2019;567(7748):414–9.
28. Liu Z, Wang L, Guo C, Liu L, Jiao D, Sun Z, et al. TTN/OBSCN 'Double-Hit' predicts favourable prognosis, 'immune-hot' subtype and potentially better immunotherapeutic efficacy in colorectal cancer. J Cell Mol Med. 2021;25(7):3239–51.
29. Liu X, Liu J, Xiao W, Zeng Q, Bo H, Zhu Y, et al. SIRT1 Regulates N -Methyladenosine RNA Modification in Hepatocarcinogenesis by Inducing RANBP2-Dependent FTO SUMOylation.

Hepatology. 2020;72(6):2029–50.
30. Zhang S, Zhou D. Role of the transcriptional coactivators YAP/TAZ in liver cancer. Curr Opin Cell Biol. 2019;61:64–71.
31. Giovannini C, Fornari F, Piscaglia F, Gramantieri L. Notch Signaling Regulation in HCC: From Hepatitis Virus to Non-Coding RNAs. Cells. 2021;10(3).
32. David CJ, Massagué J. Contextual determinants of TGFβ action in development, immunity and cancer. Nat Rev Mol Cell Biol. 2018;19(7):419–35.
33. Fiskus W, Wang Y, Joshi R, Rao R, Yang Y, Chen J, et al. Cotreatment with vorinostat enhances activity of MK-0457 (VX-680) against acute and chronic myelogenous leukemia cells. Clin Cancer Res. 2008;14(19):6106–15.
34. Jin X, Mo Q, Zhang Y, Gao Y, Wu Y, Li J, et al. The p38 MAPK inhibitor BIRB796 enhances the antitumor effects of VX680 in cervical cancer. Cancer Biol Ther. 2016;17(5):566–76.
35. Giles FJ, Swords RT, Nagler A, Hochhaus A, Ottmann OG, Rizzieri DA, et al. MK-0457, an Aurora kinase and BCR-ABL inhibitor, is active in patients with BCR-ABL T315I leukemia. Leukemia. 2013;27(1):113–7.
36. Yao R, Zheng J, Zheng W, Gong Y, Liu W, Xing R. VX680 suppresses the growth of HepG2 cells and enhances the chemosensitivity to cisplatin. Oncol Lett. 2014;7(1):121–4.
37. Lansing TJ, McConnell RT, Duckett DR, Spehar GM, Knick VB, Hassler DF, et al. In vitro biological activity of a novel small-molecule inhibitor of polo-like kinase 1. Mol Cancer Ther. 2007;6(2):450–9.
38. Didier C, Cavelier C, Quaranta M, Demur C, Ducommun B. Evaluation of Polo-like Kinase 1 inhibition on the G2/M checkpoint in Acute Myelocytic Leukaemia. Eur J Pharmacol. 2008;591(1–3):102–5.

Figures

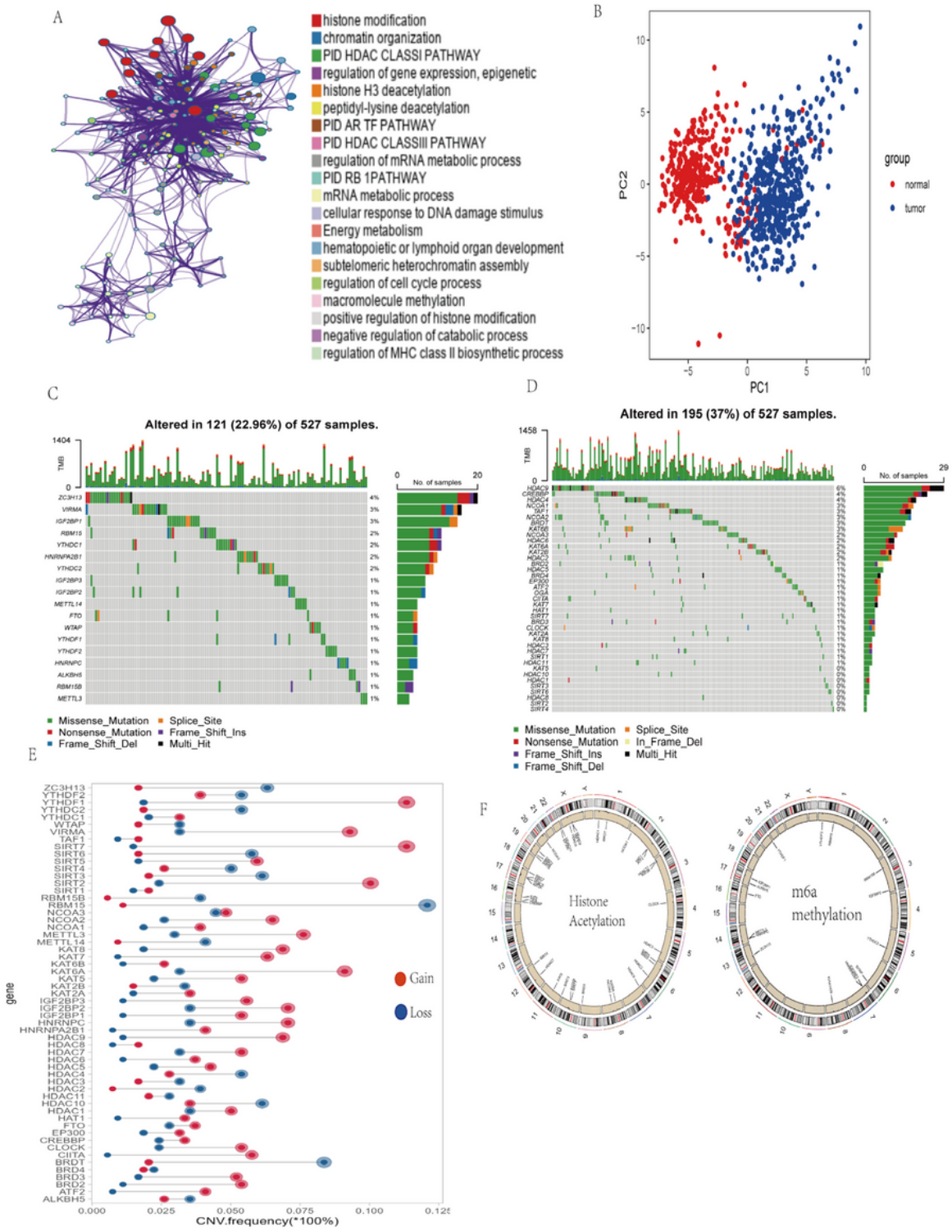

Figure 1

The landscape of genetic alterations of regulators in LUAD. (A) Functional annotations of 57 regulators analyzed by the Metascape enrichment tool. Cluster annotations are shown in the color code. (B) Principal component analysis was performed on 57 regulators to distinguish tumor and normal samples in TCGA and GTEx. (C) The mutation frequency of 18 m6a regulators in TCGA-LUAD cohort. Each column represents individual patients. The barplot on top shows TMB, and the numbers on the right display the

mutation frequency of each regulator. The barplot on the right shows the proportion of each variation type. (D) The mutation frequency of 39 histone acetylation regulators in TCGA-LUAD cohort. (E) The copy number variation (CNV) frequency of 57 regulators is common in TCGA-LUAD. This column represents the frequency of alteration. Deletion frequencies are light blue dots; amplification frequencies are dark red dots.(F) The location of CNV alteration of m6A regulators and m6a regulators on 23 chromosomes in TCGA-LUAD cohort.

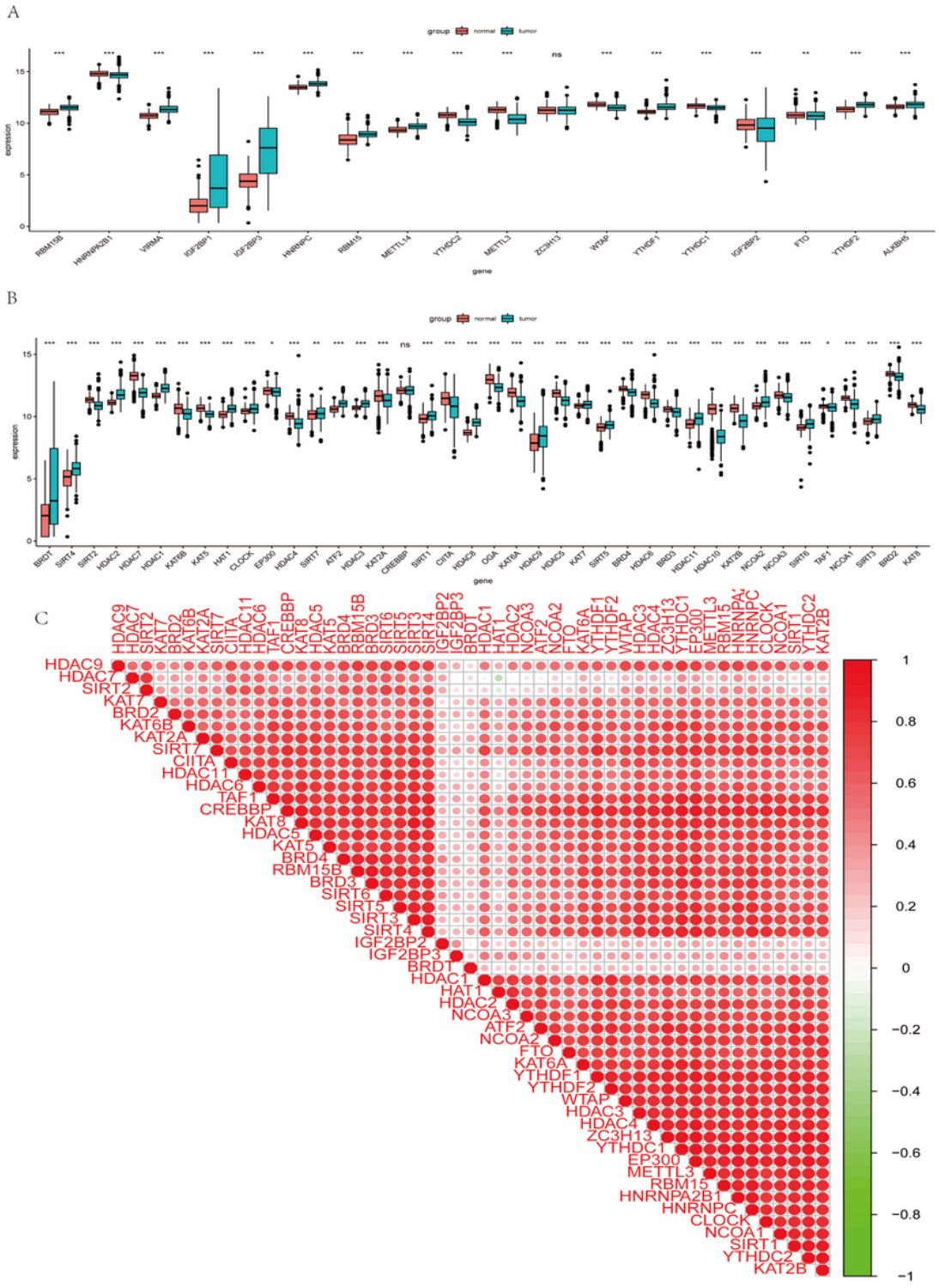

Figure 2

Expression and relevance of regulators. (A)Expression of 18 m6A methylation regulator in TCGA and GTEx cohorts in normal and tumor.(B)Expression of 39 histone acetylation regulators in TCGA and GTEx cohorts in normal and tumor.(C)Correlation analysis of m6A methylation regulators with histone acetylation regulators. Red represents positive correlation, green represents negative correlation.

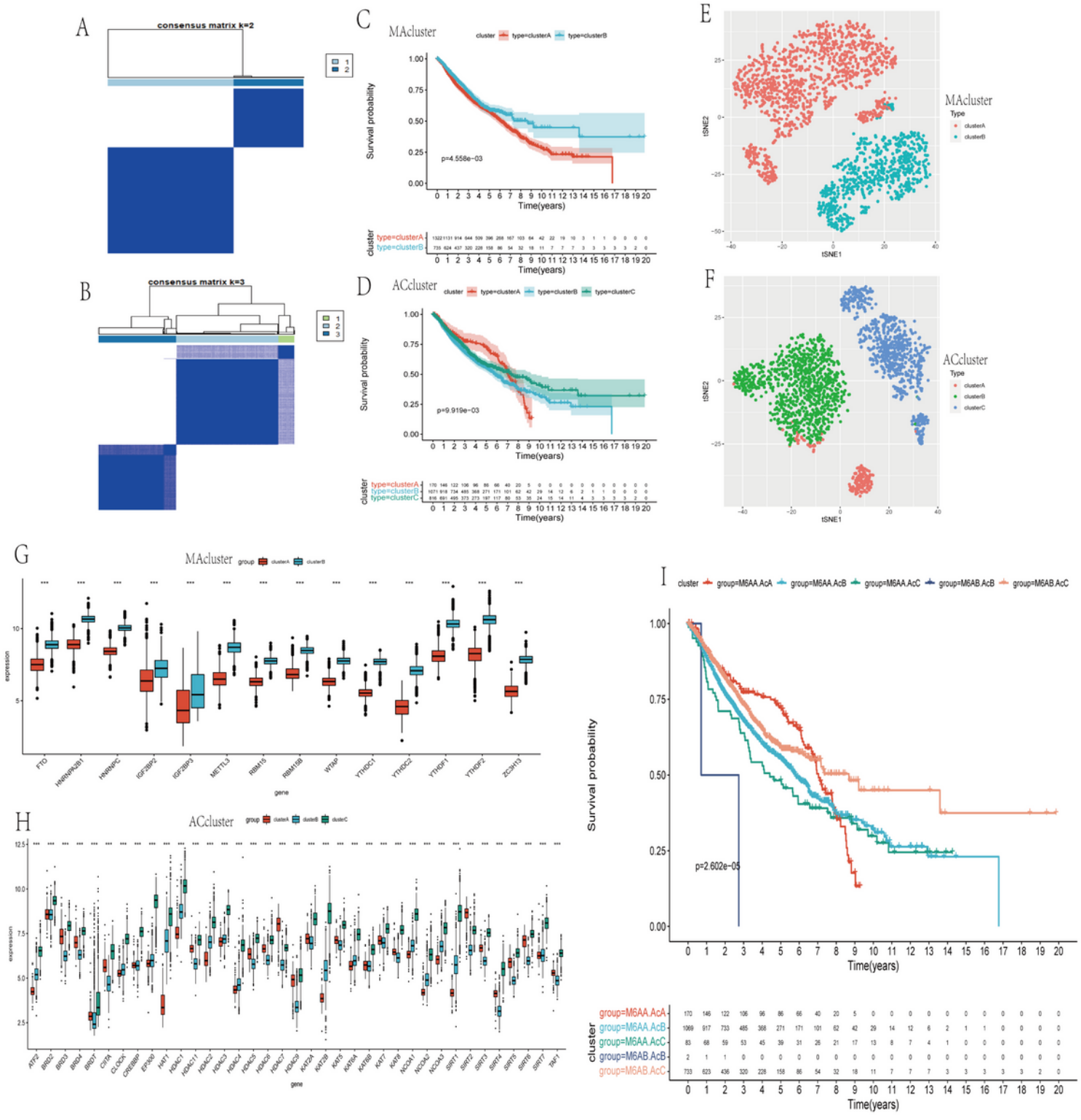

Figure 3

modification patterns in LUAD. (A)Consensus matrix of m6A methylation for 2057 samples.(B)Consensus matrix of histone acetylation for 2057 samples.(C)Survival analysis of m6A methylation modification patterns.(D)Survival analysis of histone acetylation modification patterns.(E)Principal component analysis was performed on 14 m6A methylation regulators to distinguish methylation modification patterns.(F)Principal component analysis was performed on 37 histone acetylation regulators to distinguish histone acetylation modification patterns.(G)Expression of m6A regulators in the m6A methylation modification pattern.(H)Expression of histone acetylation regulators in the histone acetylation modification pattern.(I)Survival analysis of mixed groupings of m6A methylation and histone acetylation. Asterisks represent statistical p-values (*p < 0.05; **p < 0.01; ***p < 0.001).M6AA.AcA: A grouping consisting of common samples of MAclusterA and ACclusterA groups. M6AA.AcB, M6AA.AcC, M6AB.AcB and M6AB.AcC are also grouped in the same way.

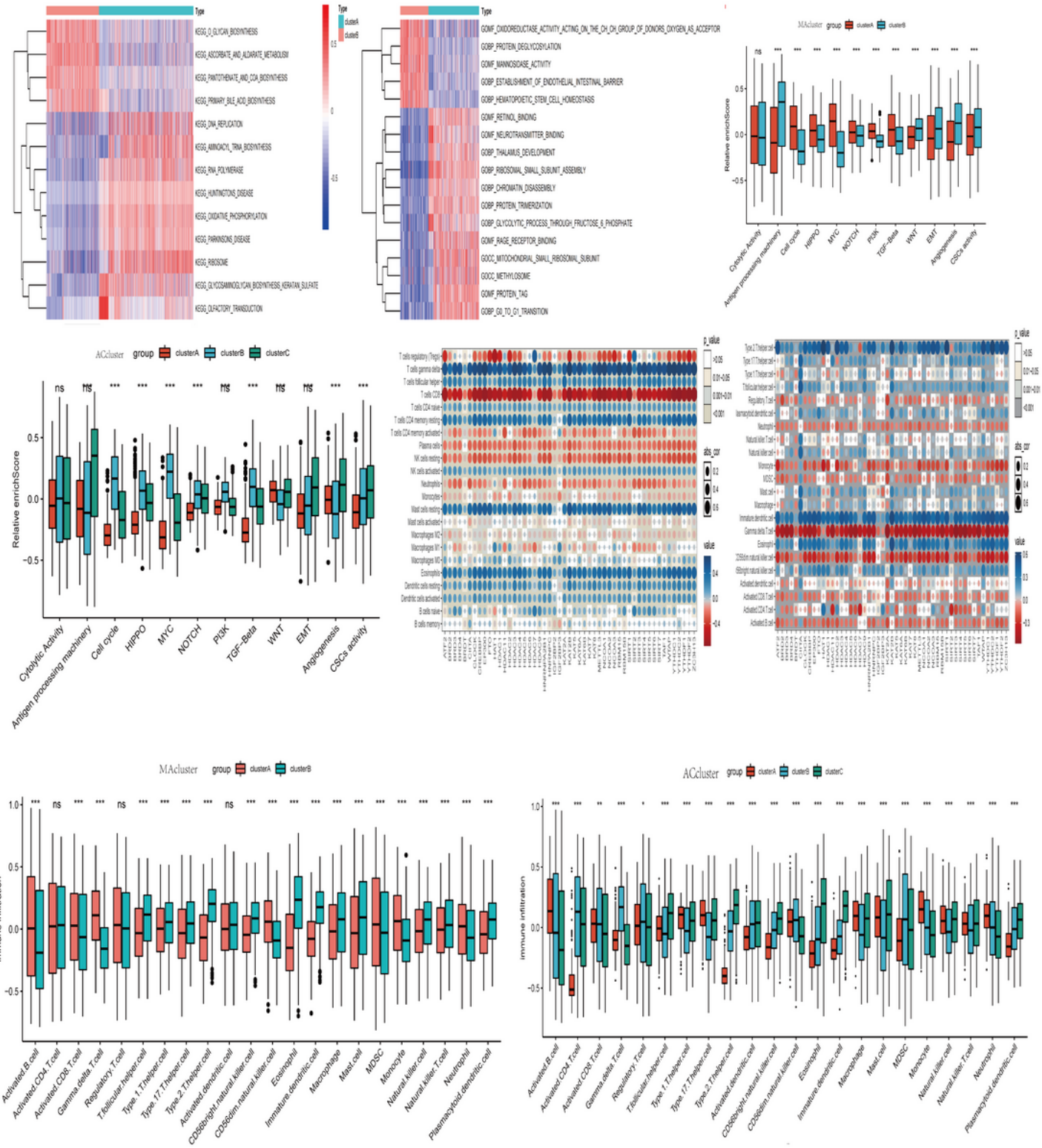

Figure 4

Infiltration characteristics and biological features of TME cells in different dilution patterns. (A B)GSVA enrichment analysis showing the activation status of the KEGG (A) vs. GO (B) biological pathway between MAclusterA-B. Red and blue colors indicate the activation and inhibition states, respectively, and are visualized by heat map.(C,D)Differences in oncogenic pathways in two different MAcluster groups(C) and three ACcluster groups(D).(E,F)Correlation analysis of regulatory factors and immune cells, the size

of the dots represents the value of the correlation coefficient, blue and red represent positive and negative correlations, respectively.(H,G)The abundance of immune cells in different groups of MAcluster(H) and ACcluster(G). Asterisks represent statistical p-values (*p < 0.05; **p < 0.01; ***p < 0.001).

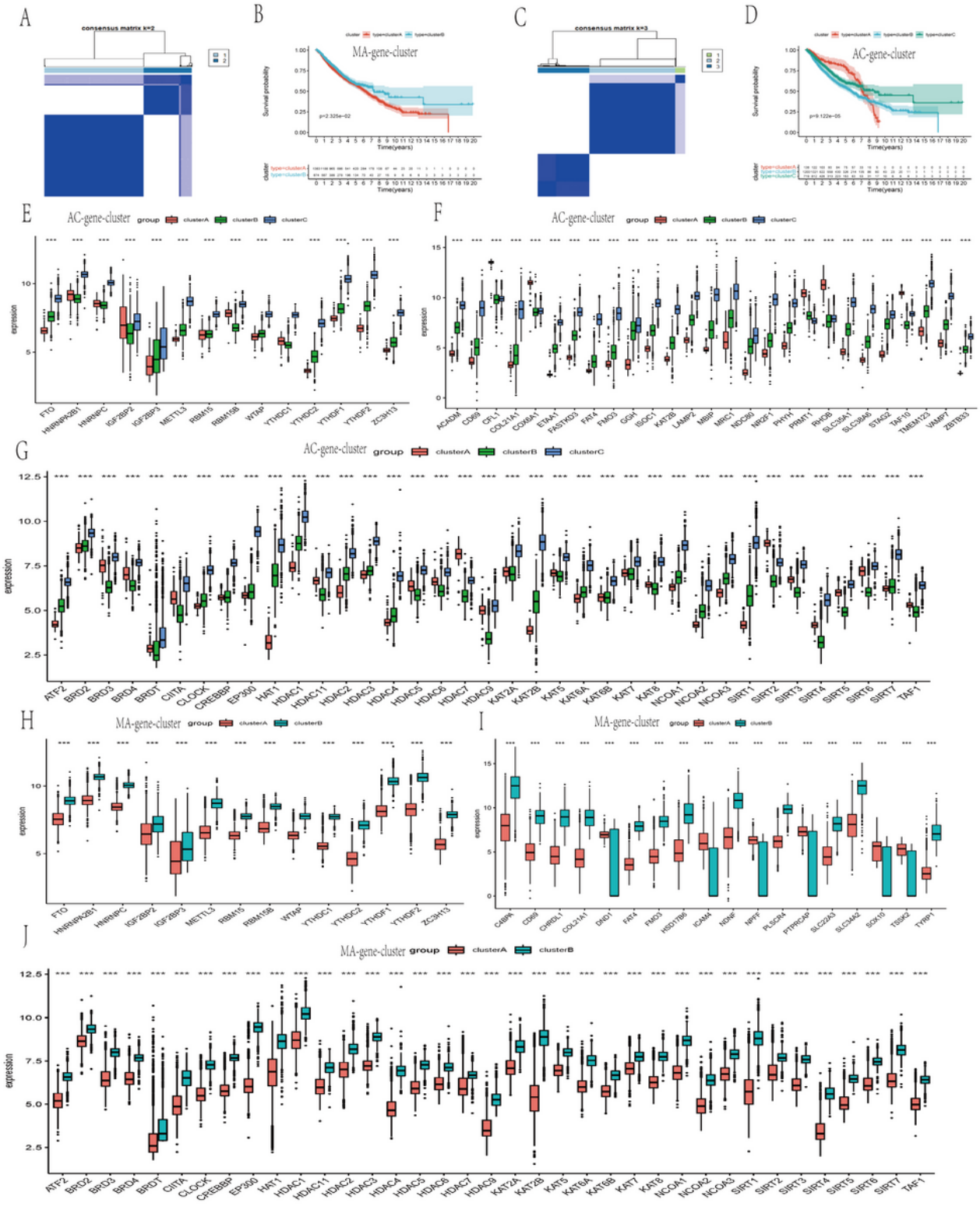

Figure 5

Genomic subtyping of differentially expressed genes that can affect the prognosis of cancer patients by unsupervised clustering analysis. (A B)Consensus matrix of DEGs based on m6A methylation grouping(A) and the corresponding survival analysis(B).(C,D) Consensus matrix of DEGs based on m6A methylation grouping(C) and the corresponding survival analysis(D).(E-G)Expression of different histone acetylation gene cluster genes: m6A regulators(E), DEGs(F), histone acetylation regulators(G).(H-J)Expression of different m6A methylation gene cluster genes: m6A regulators(H), DEGs(I), histone acetylation regulators(J). Asterisks represent statistical p-values (*p < 0.05; **p < 0.01; ***p < 0.001).

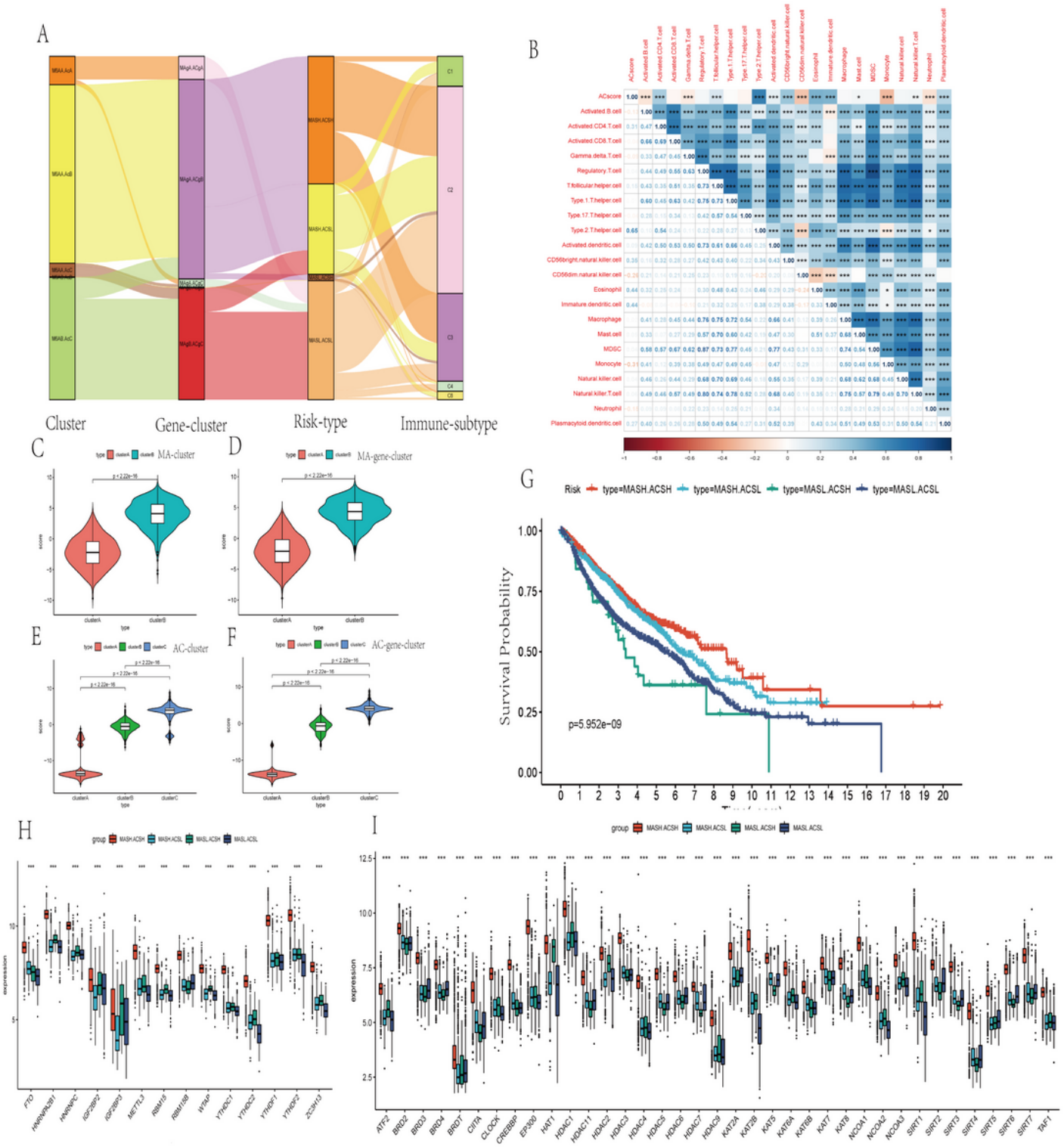

Figure 6

Digital Model for Individual Lung Adenocarcinoma Patients.**(A)**Alluvial plots showing changes in clusters, gene clusters, risk groupings, and immune subtypes.**(B)** Correlation analysis of ACscore and immune cells.**(C,D)**Levels of MAscore in MAcluster(C), MA-gene-cluster (D)groups.**(E,F)**Levels of ACscore in ACcluster(E), AC-gene-cluster (F)groups.**(G)**Survival analysis of mixed groupings of MAscore and ACscore.**(H,I)**Expression of m6A methylation regulators(H) and s histone acetylation regulators(I) in mixed subgroups. Asterisks represent statistical p-values (*$p < 0.05$; **$p < 0.01$; ***$p < 0.001$).MASH.ACSH: A grouping consisting of common samples from the MAscore high group and the ACscore group.MASH.ACSL,MASL,ACSH and MASL,ACSL are also grouped in the same way.

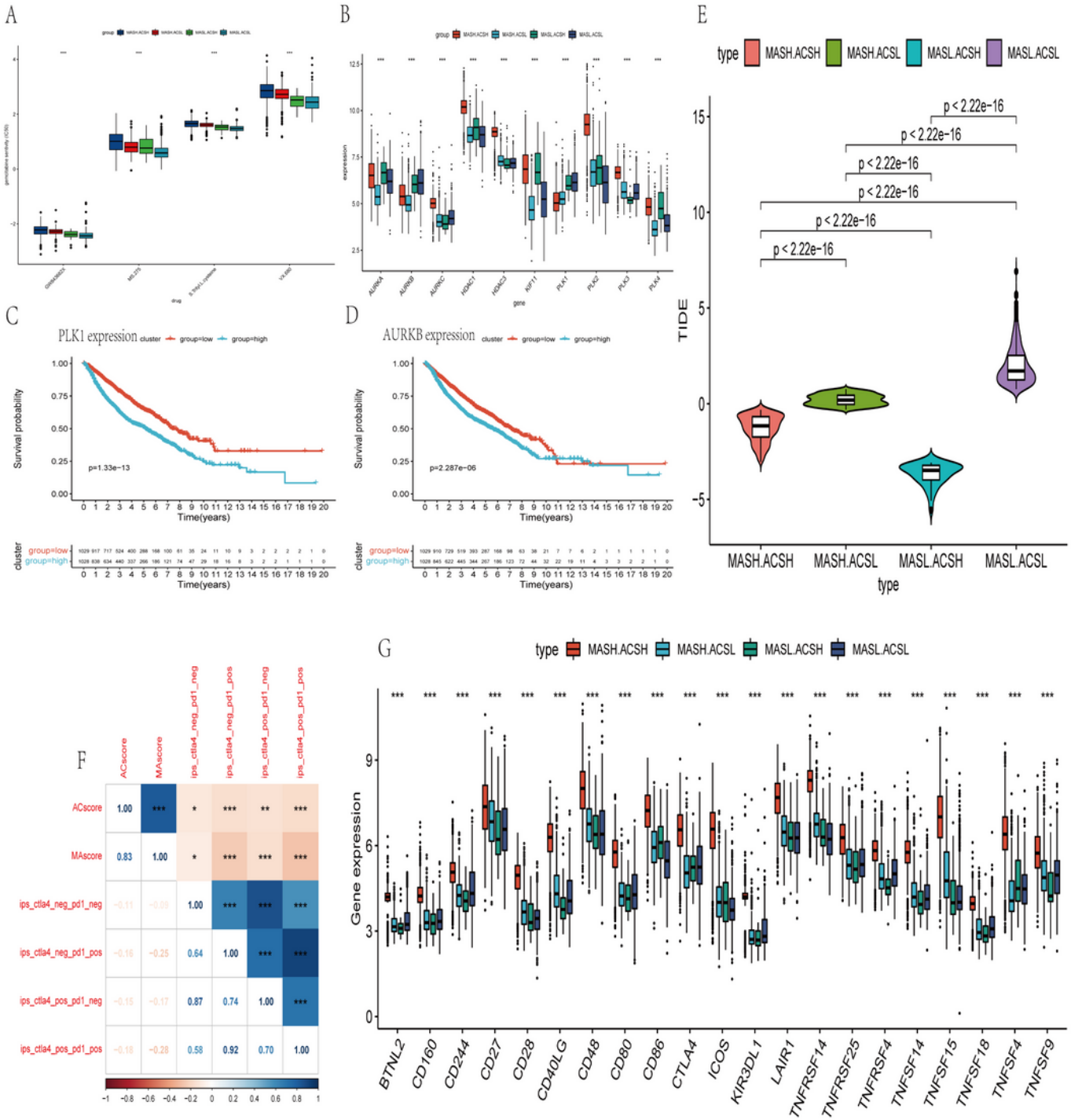

Figure 7

Screening of targeted therapeutic agents and prediction of ICI treatment responsiveness.**(A)**Sensitivity prediction of four drugs in score subgroups.**(B)** Expression of target genes of drugs in each group. **(C,D)**Survival analysis confirmed the effect of PLK1(C)/AURKB(D) expression on survival.**(E)**TIDE scores for each scoring group.**(F)**Correlation analysis of MAscore, ACscore and IPS in TCGA-LUAD cohort. **(G)**Expression of immune checkpoints in each scoring subgroup. Asterisks represent statistical p-values

(*$p < 0.05$; **$p < 0.01$; ***$p < 0.001$).MASH.ACSH: A grouping consisting of common samples from the MAscore high group and the ACscore group.MASH.ACSL,MASL,ACSH and MASL,ACSL are also grouped in the same way.

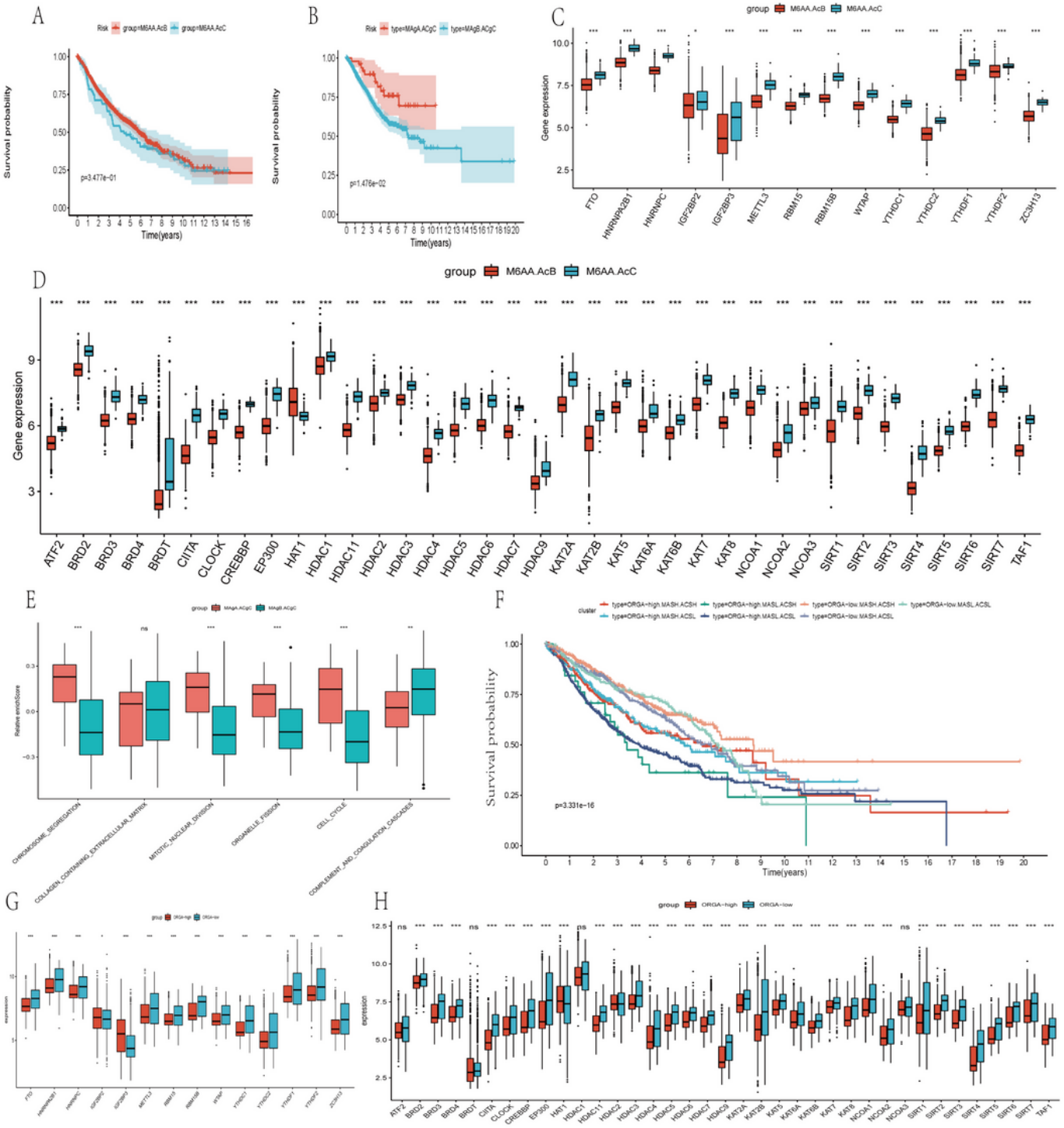

Figure 8

Organelle fission contributes to the isoform grouping of m6A methylation and histone acetylation. (A)Survival analysis of M6AA.AcB and M6AA.AcC.(B)Survival analysis of MAgA.ACgC and MAgB.ACgC. (C,D)Expression of m6A regulators(C) and histone acetylation regulators(D) between M6AA.AcB and M6AA.AcC groups.(E)Six biological characteristics differed between MAgA.ACgC and MAgB.ACgC groups.(F)Survival analysis based on a mixed group of MAscore, ACscore and Organelle fission. (G,H)Differential expression of m6A methylation regulators(G) and histone acetylation regulators(H) in high and low activity groupings of Organelle fission. Asterisks represent statistical p-values (*p < 0.05; **p < 0.01; ***p < 0.001).MASH.ACSH: A grouping consisting of common samples from the MAscore high group and the ACscore group.MASH.ACSL,MASL,ACSH and MASL,ACSL are also grouped in the same way.

Supplementary Files

This is a list of supplementary files associated with this preprint. Click to download.

- Supplementtable.xlsx
- supplementfigure.pdf